JOC Article

Tuning the Redox Chemistry of 4-Benzoyl-*N*-methylpyridinium Cations through Para Substitution. Hammett Linear Free Energy Relationships and the Relative Aptitude of the Two-Electron Reduced Forms for H-Bonding

Nicholas Leventis,* Abdel-Monem M. Rawaswdeh, Guohui Zhang, Ian A. Elder, and Chariklia Sotiriou-Leventis*

Department of Chemistry, University of Missouri−Rolla, Rolla, Missouri 65409

leventis@umr.edu; cslevent@umr.edu

Received July 23, 2002

In anhydrous CH_3CN a series of nine 4-(4-substituted-benzoyl)-*N*-methylpyridinium cations (substituent: $-OCH_3$, $-CH_3$, $-H$, $-SCH_3$, $-Br$, $-C\equiv CH$, $-CHO$, $-NO_2$, and $-^+S(CH_3)_2$) demonstrate two chemically reversible, well-separated one-electron (1-e) reductions in the same potential range as other main stream redox catalysts such as quinones and viologens. Hammett linear free energy plots yield excellent correlation between the $E_{1/2}$ values of both waves and the substituent constants σ_{p-X}. The reaction constants for the two 1-e reductions are $\rho_1 = 2.60$ and $\rho_2 = 3.31$. The lower ρ_1 value is associated with neutralization of the pyridinium ring, and the higher ρ_2 value with the negative charge developing during the 2nd-e reduction. Structure−function correlations point to a purely inductive role for substitution in both 1-e reductions. The case of the 4-(4-nitrobenzoyl)-*N*-methylpyridinium cation is particularly noteworthy, because the 4-nitrobenzoyl moiety undergoes reduction *before* the 2nd reduction of the 4-benzoyl-*N*-methylpyridinium system. Correlation of the third wave of this compound with the 2nd-e reduction of the others yields $\sigma_{p-NO_2^{\bullet -}} = -0.97 \pm 0.02$, thus placing the $-NO_2^{\bullet -}$ group among the strongest electron donors. Solvent deuterium isotope effects and maps of the electrostatic potential (via PM3 calculations) as a function of substitution support that 2-e reduced forms develop H-bonding with proton donors (e.g., CH_3-OH) via the O-atom. The average number of CH_3OH molecules entering the H-bonding association increases with e-donating substituents. H-bonding shifts the 2nd reduction wave closer to the first one. This has important practical implications, because it increases the equilibrium concentration of the 2-e reduced form from disproportionation of the 1-e reduced form.

Introduction

Several of the best-known chemically reversible redox-active species contain the quaternized pyridinium system. Notable examples include the NAD^+/NADH couple that functions as an electron-transfer catalyst in the respiratory chain,[1] and the various viologens (*N*,*N*′-diquaternized 4,4′-bipyridinium salts),[2] which have been employed widely as redox mediators,[3] electrochromic materials,[4,5] electron-transfer quenchers,[6] and as redox probes in self-assembled monolayers,[7] dendrimers,[8] silicates,[9] zeolites,[10] and semiconductors.[11]

Similarly, it has been found that 4-acyl-, 4-carboxy-, 4-carbomethoxy-, 4-cyano-, and 4-benzoyl-*N*-alkylpyridinium cations may also undergo reversible one electron

(1) Lehninger, A. L. *Biochemistry*, 2nd ed.; Worth Publishers: New York, 1978; p 494.

(2) Monk, P. M. S. *The Viologens: Physicochemical Properties, Synthesis and Applications of the Salts of 4,4′-Bipyridine*; John Wiley and Sons: New York, 1998.

(3) (a) Leventis, N.; Chen, M.; Liapis, A. I.; Johnson, J. W.; Jain, A. *J. Electrochem. Soc.* **1998**, *145*, L55. (b) Leventis, N.; Gao, X. *J. Phys. Chem. B* **1999**, *103*, 5832.

(4) (a) Imahori, H.; Norieda, H.; Nishimura, Y.; Yamazaki, I.; Higuchi, K.; Kato, N.; Motohiro, T.; Yamada, H.; Tamaki, K.; Arimura, M.; Sakata, Y. *J. Phys. Chem. B* **2000**, *104*, 1253. (b) Fukushima, M.; Tatsumi, K.; Tanaka, S.; Nakamura, H. *Environ. Sci. Technol.* **1998**, *32*, 3948. (c) Moretto, L. M.; Ugo, P.; Zanata, M.; Guerriero, P.; Martin, C. R. *Anal. Chem.* **1998**, *70*, 2163. (d) Yuan, R.; Watanabe, S.; Kuwabata, S.; Yoneyama, H. *J. Org. Chem.* **1997**, *62*, 2494. (e) Nakamura, Y.; Kamon, N.; Hori, T. *Chem. Soc. Jpn.* **1989**, *62*, 551.

(5) Bookbinder, D. C.; Wrighton, M. S. *J. Electrochem. Soc.* **1983**, *130*, 1080.

(6) (a) Konishi, T.; Fujitsuka, M.; Ito, O.; Toba, Y.; Usui, Y. *J. Phys. Chem. A* **1999**, *103*, 9938. (b) Zahavy, E.; Seiler, M.; Marx-Tibbon, S.; Joselevich, E.; Willner, I.; Dürr, H.; O'Connor, D.; Harriman, A. *Angew. Chem., Int. Ed. Engl.* **1995**, *34*, 1005. (c) Inada, T. N.; Miyazawa, C. S.; Kikuchi, K.; Yamauchi, M.; Nagata, T.; Takahashi, Y.; Ikeda, H.; Miyahi, T. *J. Am. Chem. Soc.* **1999**, *121*, 7211. (d) Warren, J. T.; Chen, W.; Johnston, D. H.; Turro, C. *Inorg. Chem.* **1999**, *38*, 6187. (e) Borsarelli, C. D.; Braslavsky, S. E. *J. Phys. Chem. A* **1999**, *103*, 1719.

(7) (a) Leventis, N.; Sotiriou-Leventis, C.; Chen, M.; Jain, A. *J. Electrochem. Soc.* **1997**, *144*, L305. (b) Li, J.; Chen, G.; Dong, S. *Electroanalysis* **1997**, *9*, 834. (c) Tang, X.; Schneider, T. W.; Walker, J. W.; Buttry, D. A. *Langmuir* **1996**, *12*, 5921. (d) Tang, X.; Schneider, T.; Buttry, D. A. *Langmuir* **1994**, *10*, 2235. (e) Katz, E.; Itzhak, N.; Willner, I. *Langmuir* **1993**, *9*, 1392. (f) De Long, H. C.; Buttry, D. A. *Langmuir* **1992**, *8*, 2491. (g) Creager, S. E.; Collard, D. M.; Fox, M. A. *Langmuir* **1990**, *6*, 1617. (h) Lee, K. A. B. *Langmuir* **1990**, *6*, 709. (i) De Long, H. C.; Buttry, D. A. *Langmuir* **1990**, *6*, 1319.

(8) (a) Vögtle, F.; Plevoets, M.; Nieger, M.; Azzellini, G. C.; Credi, A.; De Cola, L.; De Marchis, V.; Venturi, M.; Balzani, V. *J. Am. Chem. Soc.* **1999**, *121*, 6290. (b) Jockusch, S.; Ramirez, J.; Sanghvi, K.; Nociti, R.; Turro, N. J.; Tomalia, D. A. *Macromolecules* **1999**, *32*, 4419. (c) Pollak, K. W.; Leon, J. W.; Fréchet, J. M. J.; Maskus, M.; Abruña, H. D. *Chem. Mater.* **1998**, *10*, 30.

10.1021/jo020489+ CCC: $22.00
Published on Web 09/25/2002

(1-e) reduction.[12] In that context, the reduced forms of 4-acyl- and 4-benzoylpyridinium cations are stable species, for which ESR spectroscopy, dipole moment studies, and chemical trapping point toward a pyridinium-based radical.[13,14] On the contrary, it is noteworthy that the 1-e reduction of *nonquaternized* 4-acetylpyridine is followed by dimerization to the corresponding pinacol.[15]

Recently, we reported that in anhydrous CH_3CN, the 4-benzoyl-*N*-methylpyridinium cation undergoes *two* successive, well-separated ($\Delta E_{1/2} > 0.6$ V), chemically reversible 1-e reductions, generally in the same potential range as quinones and main stream viologens.[16] It was discovered further that the 2-e reduced form develops hydrogen (H-) bonding with weak protic acids. At time scales much longer (e.g., 400 s) than the time scale of a typical cyclic voltammetric scan at 0.1 V s^{-1} (20−30 s), H-bonded adducts with alcohols or water undergo proton transfer and yield carbinols. Meanwhile, owing to disproportionation of the red 1-e reduced form, very small concentrations ($<10^{-10}$ M) of the yellow 2-e reduced form are always present in equilibrium with the former.[14,16] Therefore, under rigorous exclusion of potential proton donors the 4-benzoyl-*N*-methylpyridinium cation may be suitable as a redox catalyst,[16] a photoinduced electron-transfer acceptor,[12,17] or an electrochromic material,[18] in applications where the 1-e reduced form must be generated and survive millions of cycles over a very long period of time.[19]

The similar redox behavior of the 4-benzoyl-*N*-methylpyridinium system to those of quinones and viologens notwithstanding, the former class of compounds offers direct synthetic access to the strategic *para* position of the benzoyl group. Thus, nine different 4-(*p*-substituted-benzoyl)-*N*-methypyridinium cations (**1**-X) were prepared, and their redox properties were studied in parallel to those of their free bases (BP−X) both in anhydrous CH_3CN and in the presence of a typical proton donor, such as CH_3OH. The results confirm that in general, the 4-benzoyl-*N*-methylpyridinium system demonstrates two reversible 1-e reductions. Structure−function correlations via semiempirical (PM3) calculations and Hammett Linear Free Energy relationships point toward a purely inductive interaction between the substituents and the reduction sites. e-Donating substituents increase the e-density at the oxygen of the 2-e reduced form, hence its ability to associate with CH_3OH via H-bonding. In the course of these studies, it was noticed that the *p*-nitrobenzoyl moiety of **1**-NO_2 is reduced before the 4-benzoyl-*N*-methylpyridinium system uptakes its 2nd-e. Thus, by correlating the $E_{1/2}(3)$ value of **1**-NO_2 with the $E_{1/2}(2)$ values of the other **1**-X's, we have been able to report for the first time the $\sigma_{p-NO_2^{\bullet-}}$ value of $-NO_2^{\bullet-}$.

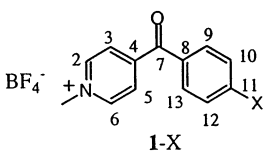

1-X

Results and Discussion

4-Benzoylpyridines have been investigated for their potential pharmacological properties.[20] So, most of our free bases have been described before,[20−24] while most BF_4^- quaternary salts and the free bases of **1**-SCH_3, **1**-CHO, and **1**-$^+S(CH_3)_2$ are new compounds. The synthetic tree of all **1**-X's is summarized in Scheme S.1 of the Supporting Information.

All redox properties (Table 1) were determined by cyclic voltammetry at 0.1 V s^{-1} in anhydrous CH_3CN/0.1 M tetrabutylammonium perchlorate (TBAP), vs ferrocene as internal standard. With the exception of **1**-NO_2 (see below), all other **1**-X's show two well-separated redox waves in analogy to **1**-H and **1**-C≡CH.[16] (A similar observation is made with the 4-acetyl-*N*-methylpyridinium cation, a typical nonbenzoyl 4-carbonylpyridinium system: see Table 1.) The cathodic-to-anodic peak current ratios, $i_{p,c}/i_{p,a}$, of both waves were determined by using the extrapolation of the decaying current of the previous wave as baseline. With the exception of the second wave of **1**-$^+S(CH_3)_2$, both waves of all other **1**-X's (and all three waves of **1**-NO_2) show chemical reversibility ($i_{p,c}/i_{p,a} \sim 1.0$; Table 1). $E_{1/2}$ values for each wave were calculated as the middle points between the cathodic and anodic peak current potentials. The peak-to-peak potential separations, ΔE_{p-p}, are comparable to the value found for the ferrocenium/ferrocene ($Fc^{\bullet+}$/Fc) couple (68 ± 3 mV).

Free bases BP−X (Table 1) generally show two reduction waves as well. With the exception of BP−Br and BP−C≡CH, all 1st waves behave as chemically revers-

(9) (a) Ruetten, S. A.; Thomas, J. K. *Langmuir* **2000**, *16*, 234. (b) Zhang, G.; Mao, Y.; Thomas, J. K. *J. Phys. Chem. B* **1997**, *101*, 7100. (c) Pfennig, B. W.; Chen, P.; Meyer, T. J. *Inorg. Chem.* **1996**, *35*, 2898.
(10) (a) Vitale, M.; Castagnola, N. B.; Ortins, N. J.; Brooke, J. A.; Vaidyalingam, A.; Dutta, P. K. *J. Phys. Chem. B* **1999**, *103*, 2408. (b) Castagnola, N. B.; Dutta, P. K. *J. Phys. Chem. B* **1998**, *102*, 1696.
(11) (a) Bavykin, D. V.; Savinov, E. N.; Parmon, V. N. *Langmuir* **1999**, *15*, 4722. (b) Logunov, S.; Green, T.; Marguet, S.; El-Sayed, M. A. *J. Phys. Chem. A* **1998**, *102*, 5652. (c) Robins, D. S.; Dutta, P. K. *Langmuir* **1996**, *12*, 402.
(12) Jones, G., II; Mabla, V. *J. Org. Chem.* **1985**, *50*, 5776.
(13) (a) Kosover, E. M.; Poziomek, E. J. *J. Am. Chem. Soc.* **1964**, *86*, 5515. (b) Grossi, L.; Minisci, F.; Pedulli, G. F. *J. Chem. Soc., Perkin Trans. 2* **1977**, 943. (c) Grossi, L.; Minisci, F.; Pedulli, G. F. *J. Chem. Soc., Perkin Trans. 2* **1977**, 948.
(14) Neta, P.; Patterson, L. K. *J. Phys. Chem.* **1974**, *78*, 2211.
(15) (a) Hermolin, J.; Kopilov, J.; Gileadi, E. *J. Electroanal. Chem.* **1976**, *71*, 245. (b) Kopilov, J.; Shatzmiller, S.; Kariv, E. *Electrochim. Acta* **1976**, *21*, 535. (c) Kopilov, J.; Kariv, E.; Miller, L. L. *J. Am. Chem. Soc.* **1977**, *99*, 3450.
(16) Leventis, N.; Elder, I. A.; Gao, X.; Bohannan, E. W.; Sotiriou-Leventis, C.; Rawashdel, A.-M. M.; Overschmidt, T. J.; Gaston, K. R. *J. Phys. Chem. B* **2001**, *105*, 3663.
(17) Shu, C.-F.; Wrighton, M. S. *Inorg. Chem.* **1988**, *27*, 4326.
(18) Yoshiike, N.; Kondo, S.; Fukai, M. *J. Electrochem. Soc.* **1980**, *127*, 1496.
(19) See for example: (a) Byker, H. J. *Proc. Electrochem. Soc.* **1994**, *94*, 2. (b) Byker, H. J. U.S. Patent, 5,128,799, 1992. (c) Byker, H. J. U.S. Patent, 4,902,108, 1990.
(20) (a) Cavallini, G.; Milla, E.; Grumelli, E.; Ravenna, F.; Grasso, I. *Farmaco, Ed. Sci.* **1958**, *12*, 853. (b) Breen, M. P.; Bojanowski, E. M.; Cipolle, R. J.; Dunn, W. J., III; Frank, E.; Gearien, J. E. *J. Pharm. Sci.* **1973**, *62*, 847. (c) McCaustland, D. J.; Chien, P.-L.; Burton, W. H.; Cheng, C. C. *J. Med. Chem.* **1974**, *17*, 993. (d) Högberg, T.; Ulff, B.; Renyi, A. L.; Ross, S. B. *J. Med. Chem.* **1981**, *24*, 1499. (e) Bäckvall, J.-E.; Nordberg, R. E.; Nyström, J.-E.; Högberg, T.; Ulff, B. *J. Org. Chem.* **1981**, *46*, 3479. (f) Earley, J. V.; Gilman, N. W. *Synth. Commun.* **1985**, *15*, 1271. (g) Carvalho, I.; Miller, J. *Heterocycl. Commun.* **1995**, *1*, 403. (h) Takemoto, M.; Yamamoto, Y.; Achiwa, K. *Chem. Pharm. Bull.* **1996**, *44*, 853.
(21) (a) Wolffenstein, R.; Hartwich, F. *Chem. Ber.* **1915**, *48*, 2043. (b) Mirek, J. *Zesz. Nauk. Uniw. Jagiellon., Pr. Chem.* **1965**, *10*, 61; *Chem. Abstr.* **1967**, *66*, 37125h. (c) Carmellino, M. L.; Pagani, G.; Pregnolato, M.; Terreni, M. *Pestic. Sci.* **1995**, *45*, 227.
(22) Lieberman, S. V.; Connor, R. *Organic Syntheses*; Wiley: New York; Collect. Vol. II, p 441.
(23) Bryans, F.; Pyman, F. L. *J. Chem. Soc.* **1929**, 549.
(24) Muth, C. W.; Yang, K. E. *J. Heterocycl. Chem.* **1996**, *33*, 249.

TABLE 1. Data for the Reduction of 1-X's, Their Free Bases [BP-X's], and Compounds Used as Controls, in CH_3CN/0.1 M TBAP at 0.1 V s^{-1} (Bracketed Quantities Correspond to the Free Bases)[a]

1-X [BP-X]	σ_{p-X}[b]	$E_{1/2}(1)$	$\Delta E_{p-p}(1)$	$i_{p,c}/i_{p,a}(1)$	$E_{1/2}(2)$ [$E_{1/2}(1)$]	$\Delta E_{p-p}(2)$ [$\Delta E_{p-p}(1)$]	$i_{p,c}/i_{p,a}(2)$ [$i_{p,c}/i_{p,a}$(1	$E_{1/2}(3)$ [$E_{1/2}(2)$]	$\Delta E_{p-p}(3)$ [$\Delta E_{p-p}(2)$]	$i_{p,c}/i_{p,a}(3)$ [$i_{p,c}/i_{p,a}(2)$]
1-OCH_3	−0.27	-1.128 ± 0.003	71 ± 2	1.00	−1.754 ± 0.008	72 ± 2	1.02			
[BP-OCH_3]					[−1.982 ±0.002]	[72 ± 2]	[1.07]	[−2.56][c]	[d]	
1-CH_3	−0.14	−1.089 ± 0.001	66 ± 1	1.00	−1.725 ± 0.002	71 ± 1	1.00			
[BP-CH_3]					[−1.939 ±0.002]	[70 ± 2]	[1.08]	[−2.53][c]	[d]	
1-H	0.00	−1.068 ± 0.001	65 ± 2	1.03	−1.697 ± 0.001	74 ± 3	1.03			
[BP-H]					[−1.905 ± 0.005]	[70 ± 2]	[1.04]	[−2.52][c]	[d]	
1-SCH_3]	0.00	−1.097 ± 0.001	69 ± 2	1.06	−1.722 ± 0.007	75 ± 2	1.06			
[BP-SCH_3					[−1.908 ± 0.001]	[70 ± 1]	[1.06]	[−2.38][c]	[d]	
1-C≡CH]	0.23	−1.035 ± 0.001	68 ± 2	1.04	−1.659 ± 0.001	76 ± 2	1.05			
[BP-C≡CH					[−1.81][c]	[d]	[1.95]	[−2.27][c]	[d]	
1-Br	0.26	−1.037 ± 0.001	68 ± 1	1.01	−1.668 ± 0.003	75 ± 3	1.07			
[BP-Br]					[−1.82][c]	[d]		[−2.45][c]	[d]	
1-CHO	0.47	−0.994 ± 0.002	66 ± 1	1.02	−1.590 ± 0.001	75 ± 1	1.02	−2.48[c]		*d*
[BP-CHO]					[−1.598 ±0.001]	[65 ± 2]	[0.98]	[−1.992 ± 0.001]	[77 ± 2]	[1.00]
1-NO_2	0.78	−0.955 ± 0.001	66 ± 1	1.00	−1.367 ± 0.003	71 ± 2	1.00	−1.893 ± 0.001	83 ± 1	1.04
[BP-NO_2]					[−1.242 ± 0.002]	[66 ± 2]	[1.04]	[−1.613 ± 0.001]	[72 ± 3]	[1.04]
1-$^+S(CH_3)_2$	0.90	−0.946 ± 0.001	72 ± 1	1.12	−1.53[c]		*d*	−2.25[c]		*d*
N-MeAP$^+$ [e]		−1.110 ± 0.001	67 ± 1	1.04	−1.830 ± 0.001	74 ± 2	1.06			
[AP][e]					[−2.05][c]	[d]				
HV^{2+} [e]		−0.826 ± 0.002	67 ± 1	1.02	−1.250 ± 0.002	70 ± 2	1.12			
Ph-CHO		−2.22[c]		*d*						
Ph-NO_2		−1.548 ± 0.003	73 ± 1	1.00						
Ph-$^+S(CH_3)_2$		−2.03[c]		*d*						

[a] $E_{1/2}$ values reported vs the ferrocenium/ferrocene couple used as internal standard. [b] Taken from ref 25a, except σ_{p-SCH_3} which was taken from ref 26. [c] The $E_{1/2}$ values of chemically irreversible waves were approximated by adding 28 mV to the corresponding peak potentials. [d] Irreversible. [e] *N*-MeAP$^+$: 4-acetyl-*N*-methylpyridinium tetrafluoroborate. AP: 4-acetylpyridine. HV^{2+}: *N*,*N*'-diheptyl-4,4'-bipyridinium tetrafluoroborate. Ph-CHO: benzaldehyde. Ph-NO_2: nitrobenzene., Ph-$^+S(CH_3)_2$: dimethylphenylsulfonium tertrafuoroborate.

ible 1-e reductions, at least within the time scale of cyclic voltammetry at 0.1 V s^{-1}. With the exception of BP−CHO and BP−NO_2, the 2nd waves of the free bases are generally chemically irreversible and smaller (about half) compared with the 1st-e waves. This observation is consistent with the fact that as the 2-e reduced form of a free base diffuses out of the electrode, it reacts with free base diffusing toward the electrode yielding the pinacol dianion.[27] Meanwhile, as will become apparent by the ensuing discussion, the reversible reduction waves of BP−CHO and BP−NO_2 do not have the same origin as the waves of the rest of the free bases, as they involve reduction of the substituents. By comparison, 4-acetylpyridine shows only one chemically irreversible reduction wave.[15] Overall, it seems that the redox behavior of **1**-X's is less idiosyncratic than that of their free bases.

Figure 1A compares the voltammograms of **1**-H, its free base, and a typical viologen (*N*,*N*′-diheptyl-4,4′-bipyridinium tetrafluoroborate; HV^{2+}), which due to symmetry has only one possible reduction site, the pyridinium. Since the 1st wave of **1**-H is pyridinium based,[13,14] it correlates well and is bracketed by the two waves of HV^{2+}. The relative position of the 1st wave of **1**-H and the two waves of HV^{2+} is the result of the relative group electronegativities: pyridinium > benzoyl > reduced pyridinium. The 2nd wave of **1**-H is in the same region as the carbonyl-based 1st-e reduction of 4-benzoylpyridine. This is a general observation among all **1**-X's and their free bases (Table 1).

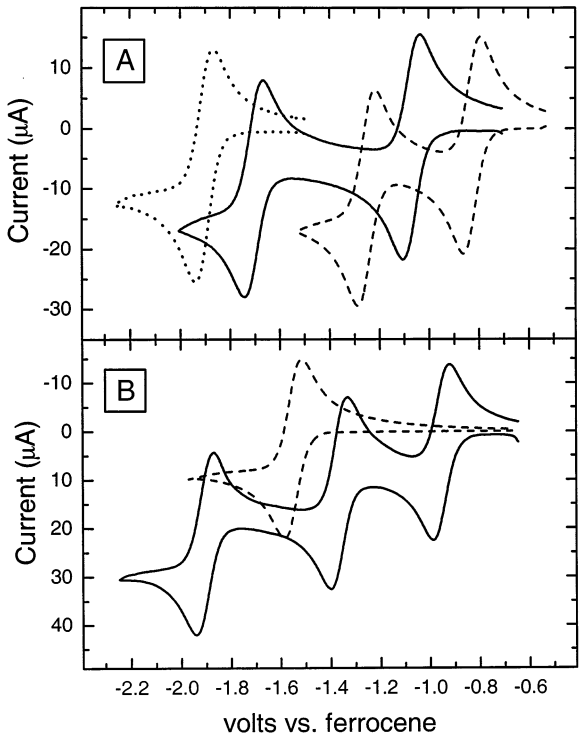

FIGURE 1. (A) Cyclic voltammetry of **1**-H (—; 2.877 mM), *N*,*N*′-diheptyl viologen (- - -; 2.878 mM), and 4-benzoylpyridine (• • •; 2.620 mM) in CH_3CN/0.1 M TBAP with a Au-disk electrode (0.0201 cm^2) at 0.1 V s^{-1}. (B) Cyclic voltammetry of **1**-NO_2 (—; 3.393 mM) and of nitrobenzene ($PhNO_2$, - - -; 6.490 mM) under the same conditions as in part A. (For $PhNO_2$, the current scale should be multiplied by a factor of "2".)

(25) Isaacs, N. *Physical Organic Chemistry*, 2nd ed.; Longman Scientific and Technical: Essex, U.K., 1995: (a) p 152; (b) p 161.
(26) Hansch, C.; Leo. A.; Taft, R. W. *Chem. Rev.* **1991**, *91*, 165.
(27) (a) Stocker, J. H.; Jenevein, R. M.; Kern, D. H. *J. Org. Chem.* **1969**, *34*, 2810. (b) Rudd, E. J.; Conway, B. E. *Trans. Faraday Soc.* **1971**, *67*, 440. (c) Nadjo, L.; Saveant, J. M. *J. Electroanal. Chem.* **1973**, *44*, 327. (d) van Tilborg, W. J. M.; Smit, C. J. *J. Roy. Neth. Chem. Soc.* **1979**, *98*, 532. (e) Swartz, J. E.; Mahachi, T. J.; Kariv-Miller, E. *J. Am. Chem. Soc.* **1988**, *110*, 3622. (f) Tanko, J. M.; Drumright, R. E. *J. Am. Chem. Soc.* **1992**, *114*, 1844. (g) Mattiello, L.; Rampazzo, L. *J. Chem. Soc., Perkin Trans.* **1993**, 2243. (h) Liotier, E.; Mousset, G.; Mousty, C. *Can. J. Chem.* **1995**, *73*, 1488.

Compound **1**-NO_2 comprises an interesting deviation from the other **1**-X's in that it shows three reversible waves (Figure 1B, solid line). The 1st wave of **1**-NO_2 falls in the same potential range as the 1st waves of the other **1**-X's; its middle wave is associated with the redox wave of nitrobenzene (Figure 1B, dashed line) and is attributed to the independent reduction of the *p*-nitrobenzoyl moiety. As expected then, BP−NO_2 shows two reversible waves that correlate with the 2nd and 3rd waves of **1**-NO_2 (Table 1). (Note that third waves are also demonstrated by **1**-CHO and **1**-$^+S(CH_3)_2$. By comparison to the reduction of benzaldehyde and of dimethylphenylsulfonium tetrafluoroborate (Table 1), those waves are assigned to the reduction of the substituents; however, since those waves are more negative than the reduction waves of the 4-benzoyl-*N*-methylpyridinium system, they do not interfere with it.)

On the basis of the above, Scheme 1 summarizes the redox processes of all **1**-X's, except **1**-NO_2. Use of [**1**-X]$^+$, [**1**-X]$^\bullet$, and [**1**-X]$^-$ emphasizes the charge/spin properties of the various redox states of the 4-benzoyl-*N*-methylpyridiium system.

SCHEME 1. The Redox Processes of the 4-Benzoyl-*N*-methylpyridinium System

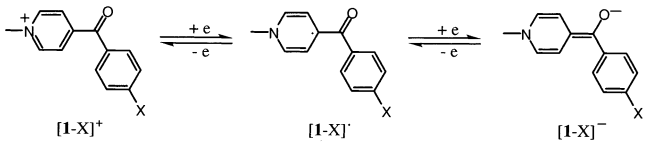

The pyridinium-based radical, [**1**-X]$^\bullet$, is consistent with literature reports on the 1-e reduced forms of other 4-substituted pyridinium salts.[13] The alternative zwitterionic species **2** for the 1-e reduced forms of **1**-X's cannot

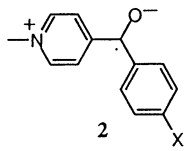

2

be derived from [**1**-X]$^\bullet$, consistent with the rules of resonance.[28a] The pyridinum ring of **2** is aromatic and planar, but there is no such guarantee for [**1**-X]$^\bullet$, for which PM3 calculations show that the geometry of N is pyramidal (Scheme 2). Species **2** conforms to the typical 1-e reduced form of a ketone,[27] and should lead to pinacolization, which has not been observed.[16]

SCHEME 2. PM3 Structures of [1-H]• and 2

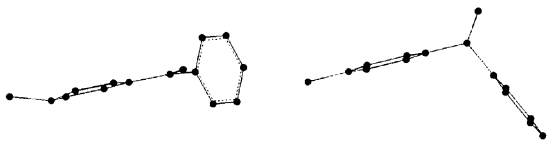

[**1**-H]· **2**

In view of possible applications, Figure 1 suggests that **1**-X's may be used in lieu of viologen. With that prospect, a better insight into the redox chemistry of **1**-X's is obtained via Hammett Linear Free Energy (HLFE) relationships in conjunction with structure/function considerations. For that analysis, it is understood that from a thermodynamic perspective, the electrode reactions of Scheme 1, referenced vs the $Fc^{\bullet+}$/Fc couple, can be written equivalently as:

$$[\mathbf{1}\text{-X}]^+ + \mathrm{Fc} \overset{K_1}{\rightleftharpoons} [\mathbf{1}\text{-X}]^\bullet + \mathrm{Fc}^{\bullet+} \quad (1)$$

$$[\mathbf{1}\text{-X}]^\bullet + \mathrm{Fc} \overset{K_2}{\rightleftharpoons} [\mathbf{1}\text{-X}]^- + \mathrm{Fc}^{\bullet+} \quad (2)$$

where K_1 and K_2 are the equilibrium constants of eqs 1 and 2, respectively. HLFE relationships for these reactions are expressed via eq 3, where ρ_1 and ρ_2 are the corresponding reaction constants, and σ_{p-X} is the sub-

$$\log [K_{1or2}/K_{1or2(X=H)}] = (\rho_{1or2})\sigma_{p-X} \quad (3)$$

stituent constant of group X in the para position. Since $RT \ln(K_{1or2}) = -\Delta G° = nFE^o_{rxn}$, eq 3 is rearranged into eq 4, where n is the number of electrons involved in the

$$E_{1/2}(1 \text{ or } 2) = [2.303RT/nF]\rho_{1or2}\sigma_{p-X} + E_{1/2}(1 \text{ or } 2 \text{ for } X = H) \quad (4)$$

redox process, F and R are the Faraday and gas constants, respectively, and T is the absolute temperature. By definition (eqs 1 and 2), the reaction standard potential, E^o_{rxn}, is the standard potential, $E°$, of the [**1**-X]$^+$/[**1**-X]$^\bullet$ couple, or the [**1**-X]$^\bullet$/[**1**-X]$^-$ couple vs the reference couple ($Fc^{\bullet+}$/Fc), and in general $E° \sim E_{1/2}$.

Deriving the electrochemical version of the Hammett equation may appear redundant, however, eq 4 is not the typical HLFE relationship used in the literature, where customarily sensitivity of redox reactions to substitution is expressed simply in terms of the slope, $dE_{1/2}/d\sigma_{p-X}$.[29,30] On the basis of eq 4, if those slopes are divided by $[2.303RT/nF]$, they yield the dimensionless ρ-values (eq 3), which allow correlation of electrode reactions with *any* other reaction (redox or otherwise) susceptible to substitution effects.

With the exception of the 2nd and 3rd waves of **1**-NO_2, both $E_{1/2}$ values of all other **1**-X's show good correlation with the substituent constants, σ_{p-X} values (Figure 2). Dividing the experimental slopes (Figure 2, legend) by 0.05916 V (the value of $2.303RT/nF$ for $n = 1$ at 25 °C) yields $\rho_1 = 2.60$ and $\rho_2 = 3.31$. Both ρ values are positive, consistent with the fact that a positive charge is neutralized and a negative charge is developing during the 1st-e and the 2nd-e reduction, respectively. On the other hand, the $E_{1/2}(1)$ values of the free bases give poor correlation with the σ_{p-X} values ($r^2 = 0.908$; $\rho_{FB} = 7$). Introducing the σ^- value for −CHO (1.03[26]) yields a much better

(28) Smith, M. B.; March, J. *March's Advanced Organic Chemistry, Reactions, Mechanisms and Structure*, 5th ed.; John Wiley and Sons: New York, 2001:. (a) p 41; (b) p 99.

(29) Zuman, P. *Substituent Effects in Organic Polarography*; Plenum Press: New York, 1967; Chapters 1 and 2.

(30) For more recent examples see: (a) Sauro, V. A.; Workentin, M. S. *J. Org. Chem.* **2001**, *66*, 831. (b) Connelly, N. G.; Davis, P. R. G.; Harry, E. E.; Klangsinsirikul, P.; Venter, M. *J. Chem. Soc., Dalton Trans.* **2000**, 2272. (c) Aguilar-Martinez, M.; Cuevas, G.; Jimenez-Estrada, M.; Conzalez, I.; Lotina-Hennsen, B.; Macias-Ruvalcaba, N. *J. Org. Chem.* **1999**, *64*, 3684.

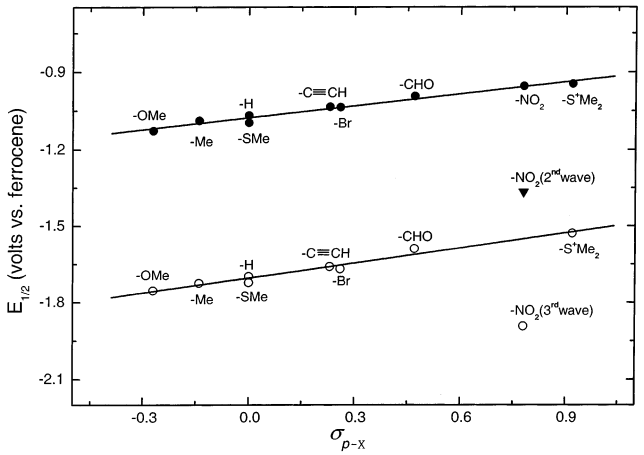

FIGURE 2. Hammett plots for the 1st-e reduction (dark circles; slope = 0.154 V; intercept = −1.077 V; correlation (r^2) = 0.971) and the 2nd-e reduction (open circles; slope = 0.196 V; intercept = −1.704; correlation (r^2) = 0.971) of the *p*-substituted-4-benzoyl-*N*-methylpyridinium cations (**1**-X's) of Table 1. The dark triangle corresponds to the 1-e reduction of the *p*-nitrobenzoyl moiety of **1**-NO_2 (refer to the middle wave in Figure 1B).

correlation (r^2 = 0.993; ρ_{FB} = 5.04), although the 2nd wave of BP−NO_2 never correlates well with the other free bases (see Figure S.1 in the Supporting Information). The ρ values reflect the ability of the core to transmit electronic effects to the reaction site, and may have both inductive and resonance contributions.[25b] Overall, (a) the good correlation of **1**-X's with the "primitive" σ_{p-X} values, (b) the improved Hammett correlation of BP-X's by introducing σ^- values, and (c) the fact that $\rho_{FB} > \rho_1, \rho_2$ all corroborate for enhanced resonance effects in the free bases and their lack thereof from **1**-X's. A satisfactory justification for this conclusion relies on structural considerations.

According to semiempirical (PM3) calculations (Table 2), the dihedral angle between the carbonyl and the *p*-substituted-phenyl group of the free bases suggests a variable degree of possible resonance interaction between the substituent and the carbonyl group (i.e., the site of the 1st-e reduction). On the contrary, the carbonyl group of all **1**-X's is nearly orthogonal to the pyridinium group. Furthermore, after the 1st-e reduction (Scheme 2) or after the 2nd-e reduction (Table 2) both the surviving carbonyl group and the resulting enolate, respectively, are coplanar with the reduced pyridinium ring and orthogonal to the *p*-substituted-phenyl group. Therefore, in both reduction steps of **1**-X's the substitution effect is only inductive, and the fact that $\rho_2 > \rho_1$ reflects the relative distance of the reduction site from the point of substitution.[31,32] (Further supporting evidence for the proximity effect in the relative magnitude of ρ values is found in the IR stretching frequency of C=O, which is more sensitive to the value of σ_{p-X} than the frequency of N^+-CH_3.[33] See Table S.1 and Figure S.2 in the Supporting Information.)

Interestingly, the $E_{1/2}$ values of neither the 2nd nor the 3rd wave of **1**-NO_2 correlate with the $E_{1/2}$ values of the 2nd waves of the other **1**-X's (see Figure 2). This is not difficult to reconcile: the 1st-e reduction product of **1**-NO_2 is **3**, while the 2nd-e reduction takes place at the *p*-nitrobenzoyl moiety giving **4**.[34] Therefore, the 3rd-e process reduces the carbonyl group of a species where the substituent of the benzoyl group is $-NO_2^{\bullet-}$. Since there is no stereoelectronic reason (Table 2) for the reduction of **4** not to conform with the reduction of the

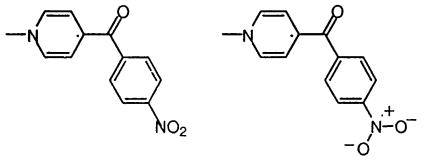

3 **4**

other [**1**-X]$^{\bullet}$'s, Figure 2 leads directly into $\sigma_{p-NO_2^{\bullet-}} = -0.97 \pm 0.02$ (for the 95% confidence limit the standard deviation should be multiplied by a factor of 2). The fact that the $\sigma_{p-NO_2^{\bullet-}}$ value is negative is not surprising: $-NO_2^{\bullet-}$ is an electron-rich group and therefore electron donating. Actually, $\sigma_{p-NO_2^{\bullet-}}$ is the most negative substituent constant we are aware of after σ_{p-S^-} (= −1.21).[26] It should be noted further that interference by reduction of the $-NO_2$ group in the same potential range as the main redox-active moiety is not something unique to these experiments. For example, it was reported recently that reduction of the $-NO_2$ group was also observed in the case of 2-(*p*-nitrophenylamine)-1,4-naphthalenedione.[30c] However, the redox potentials were not well-separated, and therefore an analysis similar to ours was not possible. By the same token, it should be noted also that the same analysis for BP−NO_2 is not possible either; although the $-NO_2$ group of that compound is reduced first (Table 1), PM3 calculations show that the *p*-($NO_2^{\bullet-}$)-phenyl ring and the reduced carbonyl, $C^{\bullet}-O^-$, are almost coplanar (dehedral = 4.48°). That supports a direct resonance interaction between $-NO_2^{\bullet-}$ and the $C^{\bullet}-O^-$ group (see **5** and **6**). Therefore, although $-NO_2^{\bullet-}$ is e-donating by induction, in the case of the 1-e reduced benzoyl moiety of BP−NO_2, it interacts directly and delocalizes the carbonyl radical. Similar arguments can be made for $[BP-CHO]^{2-}$.

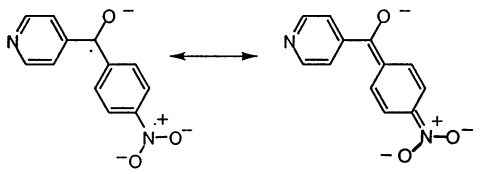

5 **6**

The strong inductive interaction—suggested by the high ρ_2 value—between the substituents and the negative charge developing upon the 2nd-e reduction of **1**-X's finds further support in Scheme 3, which shows a greatly

(31) Wells, P. R. *Linear Free Energy Relationships*; Academic Press: New York, 1968; p 12.

(32) Carey, F. A.; Sundberg, R. J. *Advanced Organic Chemistry*, 4th ed.; Part A: Structure and Mechanisms; Kluwer Academic/Plenum Publishers: New York, 2000; p 209.

(33) For example see: Berthelot, M.; Laurence, C.; Wojtkowiak, B. *Bull. Soc. Chim. Fr.* **1973**, 662.

(34) Comparison of the redox potentials of nitrobenzene (Table 1), 1-nitronaphthalene (−1.486 V vs $Fc^{\bullet+}$/Fc) and 9-nitroanthracene (ca. −1.40 V vs $Fc^{\bullet+}$/Fc; irreversible) indicates that the dominant canonical form of reduced nitro-aromatic species contains the $-NO_2^{\bullet-}$ group.

TABLE 2. Dihedral Angles of the Carbonyl Group of 1-X's and Their Free Bases, with the Pyridinium and the Phenyl Rings[a]

	1-X's[b]		free bases	
substituent (X)	$C_3-C_4-C_7-O$ pyridinium, deg	$O-C_7-C_8-C_9$ phenyl, deg	$C_3-C_4-C_7-O$ pyridinium, deg	$O-C_7-C_8-C_9$ phenyl, deg
OCH_3	87.5 (1.2)	2.7 (89.3)	40.5	86.0
CH_3	81.4 (1.2)	15.9 (89.2)	79.4	27.6
H	81.4 (1.1)	17.0 (89.2)	73.4	32.0
SCH_3	85.8 (1.2)	6.7 (89.2)	82.8	27.9
C≡CH	81.9 (1.1)	16.5 (89.1)	66.0	33.1
Br	79.4 (1.1)	22.9 (89.1)	82.9	34.4
CHO	80.2 (1.1)	23.0 (89.1)	45.1	56.1
NO_2	81.3 (0.4)	37.4 (73.9)	40.5	86.0
$^+S(CH_3)_2$	86.5	39.5		

[a] The energy minimization was carried out with PM3 semiempirical calculations. [b] The dihedral angle data after the 2nd-e reduction of the 4-benzoyl-*N*-methylpyridinium system are in parentheses. (In the case of **1**-NO_2, this refers to [**1**-$NO_2^{\bullet -}$]$^-$.)

SCHEME 3. Negative Electrostatic Potential Surfaces (via PM3 calculations) of [1-$NO_2^{\bullet -}$]$^-$, [1-H]$^-$, and [1-CHO]$^-$, at −200 au

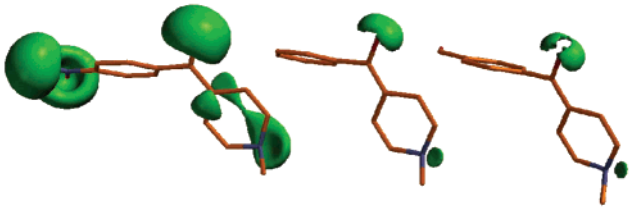

enhanced negative charge density at the enolate oxygen of [**1**-$NO_2^{\bullet -}$]$^-$ relative to [**1**-H]$^-$, which in turn has a higher negative charge density than [**1**-CHO]$^-$ in the same region. The implications of these findings are significant. According to recent evidence, weak protic acids interact selectively with the 2-e reduced forms of **1**-H and **1**-C≡CH.[16] On the basis of an analogous behavior demonstrated by quinones,[35] and spectroelectrochemical data from the reduction of **1**-H in the presence of 1-butanol,[16] the interaction between [**1**-H]$^-$ and weak protic acids was attributed to H-bonding. As it turns out, H-bonding is the preamble of an irreversible proton transfer leading to carbinols,[16] hence its study has practical significance. H-bonding has been assumed to develop at the O-atom of [**1**-X]$^-$.[16] But since para substitution modifies the negative charge density of the C=C−O$^-$ group, it should be also able to *tune* its ability to develop H-bonding. That should be considered as further evidence not only for the development of H-bonding, but also for its location.

The most dramatic effect of H-bonding between [**1**-X]$^-$'s and weak protic acids is a shift of the second cyclic voltammetric wave to more positive potentials.[16] The first wave remains unaffected.[36] This is a common observation among all **1**-X's and is demonstrated in Figure 3 by **1**-CH_3 and CH_3OH. These results cannot be attributed to a matrix effect introduced by, e.g., the small change in the dielectric constant after the addition of methanol (ϵ_{CH_3CN} = 36, ϵ_{CH_3OH} = 33), because that change would also affect the position of the first wave. Having excluded a matrix

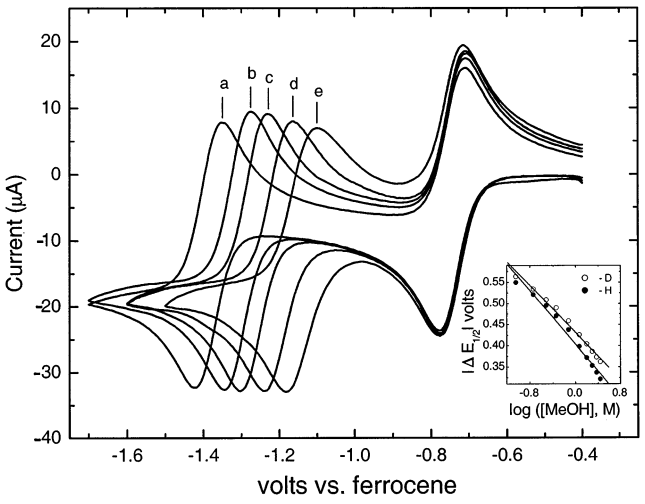

FIGURE 3. The effect of methanol on the cyclic voltammetry of **1**-CH_3 (3.310 mM) in CH_3CN/0.1 M TBAP at 0.1 V s^{-1}, using a Au-disk electrode (0.0201 cm^2). [CH_3OH]: (a) 0.0 M; (b) 0.098 M; (c) 0.244 M; (d) 0.719 M; (e) 1.615 M. Inset: Dark circles: $|\Delta E_{1/2}|$ of the two waves vs log[CH_3OH]; slope = 159 mV; intercept = 403 mV; correlation (r^2) = 0.982. Open circles: $|\Delta E_{1/2}|$ of the two waves vs log[CD_3OD]; slope = 140 mV; intercept = 431 mV; correlation (r^2) = 0.993.

effect, the fact that the first wave is not affected by CH_3OH means that [**1**-CH_3]$^\bullet$ and methanol do not interact. Also, the absence of any prewaves indicates that any possible interaction between [**1**-X]$^{+\bullet}$s and CH_3OH can be omitted safely from a mechanistic interpretation of the data of Figure 3.[37] These phenomena can be explained *only* by an interaction between the 2-e reduced form, [**1**-X]$^-$, and the proton donor (Scheme 4).[16] For large equilibrium constants, K_H, the mechanism of Scheme 4

SCHEME 4. Reduction of 1-X's in the Presence of Weak Acid Proton Donors (HA) ([1-X]$^-$ ···*m*(HA) H-Bonded Adduct)

$$[\mathbf{1}\text{-X}]^{+\bullet} + e \rightleftharpoons [\mathbf{1}\text{-X}]^{\bullet}$$

$$[\mathbf{1}\text{-X}]^{\bullet} + e \rightleftharpoons [\mathbf{1}\text{-X}]^{-}$$

$$[\mathbf{1}\text{-X}]^{-} + m\ HA \underset{K_H}{\rightleftharpoons} [\mathbf{1}\text{-X}]^{-}\cdots m(HA)$$

(35) Gupta, N.; Linschitz, H. *J. Am. Chem. Soc.* **1997**, *119*, 6384.

(36) As expected, in the presence of methanol (e.g., 50 mM) the free bases of all **1**-X's, even of those that show reversible voltammograms in anhydrous CH_3CN (Table 1), move to more positive potentials and become chemically irreversible.

TABLE 3. Slopes, Intercepts, and Other Data Related to the H-Bonded Adducts [1-X]$^-$···*m*(CH_3OH) and [1-X]$^-$···*m*(CD_3OD) Derived from the Plots of $\Delta E_{1/2}$ vs log [CH_3OH] and vs log [CD_3OD], Respectively (see Figure 3, Inset)[a]

[**1**-X]$^-$	σ_{p-X}	d$\Delta E_{1/2}$/d log [methanol][b] H (D)	$\langle m\rangle_H$[c]	$\langle m\rangle_D$[d]	intercept[b] H (D)	r^2 H (D)	$K_{H\ or\ D} \times 10^{-3}$[e] H (D)	$\Delta G°$[f] H (D)
[**1**-$NO_2^{\bullet-}$]$^-$	−0.97	243 (230)	4.11 (4)	3.89 (4)	−569 (−615)	0.998 (0.999)	1800 (300)	−8.53 (−7.46)
[**1**-OCH_3]$^-$	−0.27	172 (152)	2.91 (3)	2.57 (3)	−387 (−407)	0.993 (0.996)	11.2 (5.15)	−5.51 (−5.06)
[**1**-CH_3]$^-$	−0.14	159 (140)	2.69 (3)	2.37 (2)	−403 (−431)	0.982 (0.989)	8.90 (2.98)	−5.38 (−4.74)
[**1**-H]$^-$	0.00	159 (135)	2.69 (3)	2.28 (2)	−417 (−446)	0.987 (0.985)	3.92 (1.26)	−4.90 (−4.23)
[**1**-C≡CH]$^-$	0.23	141 (127)	2.38 (2)	2.15 (2)	−415 (−429)	0.993 (0.989)	3.49 (2.02)	−4.83 (−4.51)
[**1**-Br]$^-$	0.26	141 (125)	2.38 (2)	2.11 (2)	−415 (−433)	0.990 (0.993)	4.58 (2.27)	−4.99 (−4.57)
[**1**-CHO]$^-$	0.47	139 (117)	2.35 (2)	1.98 (2)	−393 (−418)	0.993 (0.991)	2.76 (1.04)	−4.69 (−4.11)
N-MeAP$^+$[g]		178 (166)	3.01 (3)	2.88 (3)	-480 (−488)	0.986 (0.986)	11.4 (8.30)	−5.55 (−5.21)

[a] $\Delta E_{1/2} = E_{1/2}(2) - E_{1/2}(1)$. $\Delta E_{1/2}$ reports the position of the second wave, $E_{1/2}(2)$, with respect to the fixed position of the first one, $E_{1/2}(1)$. [b] In mV. [c] $\langle m\rangle_H$ = slope of the $\Delta E_{1/2}$ vs log [CH_3OH] curve divided by 59.16 mV (see eq 6); in parentheses are the first significant figure approximations for the average (apparent) number of CH_3OH molecules participating in the H-bonded adducts. [d] As in footnote *c* for CD_3OD as "proton" donor. [e] In M^{-m}. [f] In kcal/mol. [g] Corresponding data for the 2nd-e reduction wave of *N*-methyl-4-acetylpyridinium tetrafluoroborate.

is the classic mechanism (albeit in reverse) where e-transfer is coupled with a fast equilibrium that keeps the redox-active species ([**1**-X]$^-$) in short supply.[38]

According to Scheme 4, the relationship between the electrode potential, *E*, and the ratio of the two electrode−surface concentrations, $C_{[\mathbf{1}-X]^\bullet}/C_{[\mathbf{1}-X]^-\cdots m(HA)}$, along the second wave is given at 25 °C by eq 5, where $E_{1/2}°(2)$ is

$$E = E_{1/2}°(2) + 0.059 \log K_H + m(0.059 \log[HA]) + 0.059 \log (C_{[1-X]^\bullet}/C_{[1-X]^-\cdots m(HA)}) \quad (5)$$

the half-wave potential of the second wave in the absence of HA. Consequently,[27b] the value of $E_{1/2}(2)$ of the second wave in the presence of HA is given by eq 6. Therefore,

$$E_{1/2}(2) = E_{1/2}°(2) + 0.059 \log K_H + m(0.059 \log[HA]) \quad (6)$$

the absolute slopes of the $E_{1/2}(2)$ vs log[HA] curves (e.g., Figure 3, inset), expressed in multiples of 0.059 V, represent the *apparent* (see below) number $\langle m\rangle$ of HA molecules associated with [**1**-X]$^-$ in [**1**-X]$^-$···*m*(HA). The corresponding intercepts yield the equilibrium constants K_H (eq 6). All pertinent data for several **1**-X's with CH_3OH and CD_3OD as proton donors are summarized in Table 3. Note that despite the rather high correlation coefficients (r^2), all data like those in inset in Figure 3 show distinct concave-down curvatures and slopes increasing with log [CH_3OH(D)]. This suggests that as the concentration of CH_3OH(D) increases, more methanol molecules associate with [**1**-X]$^-$.[39] In other words, there is no single value of *m* to describe the situation with each **1**-X, so the calculated *m* values should be considered only as apparent (average) values obtained by assuming only one type of [**1**-X]$^-$···*m*(methanol) species. Thereby, the utility of $\langle m\rangle$ values relies mostly with their relative values, and in this context, Figure 4 illustrates that there is strong correlation between the slopes d$E_{1/2}(2)$/d log [CH_3OH(D)] and the σ_{p-X} values. Those slopes, and therefore $\langle m\rangle_{H(D)}$, increase as the negative charge density on the enolate oxygen increases (Scheme 3). Thus, $\langle m\rangle_{H(D)}$ varies from 2 for species bearing electron-withdrawing susbstituents such as [**1**-CHO]$^-$ or [**1**-C≡CH]$^-$, to 3 for [**1**-CH_3]$^-$ and [**1**-OCH_3]$^-$, and up to 4 for [**1**-$NO_2^{\bullet-}$]$^-$.[40] Importantly, |d$E_{1/2}(2)$/d log [CH_3OH]| is always greater than |d$E_{1/2}(2)$/d log [CD_3OD]| for all **1**-X's (see Table 3 and Figure 4), meaning (eq 6) that at any given concentration $\langle m\rangle_D$ is less than $\langle m\rangle_H$. This correlation underlines the direct involvement of the −OH(D) group in the results of Figure 3, and is attributed to the steric effect resulting from the fact that the O−D bond is shorter than O−H.[41]

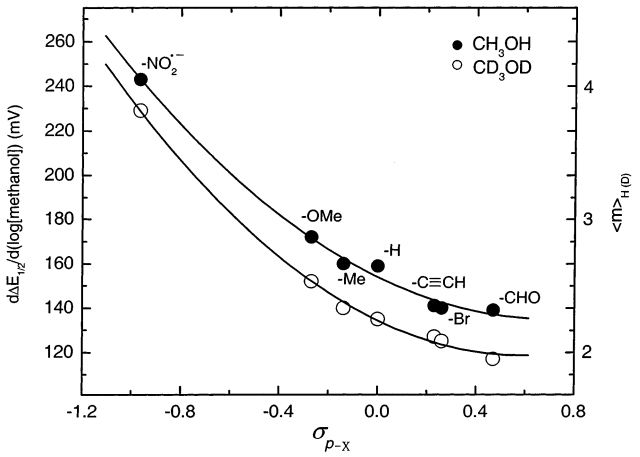

FIGURE 4. Plot of the slopes d$\Delta E_{1/2}$/d log [CH_3OH] (dark circles) and d$\Delta E_{1/2}$/d log [CD_3OD] (open circles) of the **1**-X's against Hammett substituent constants σ_{p-X}. (Data for this figure are from Table 3; refer also to the inset of Figure 3.)

The equilibrium constants, K_H (Scheme 4), are cited in Table 3 together with the corresponding standard Gibbs free energy changes, $\Delta G°$, calculated via $\Delta G° = -RT \ln K_H$. In all cases the equilibrium favors the H-bonded adduct. The $\Delta G°$ values are in the typical range for H-bonding (3−8 kcal/mol),[28b] providing independent evidence for this type of interaction. It should be noted that the energy that was calculated spectroscopically for [**1**-H]$^-$···(m = 1)(butanol) was 5.4 kcal/mol.[16] The high

(37) (a) Paduszek-Kwiatek, B.; Kalinowski, M. K. *Electrochim. Acta* **1984**, *29*, 1439. (b) Kwiatek, B.; Kalinowski, M. K. *Aust. J. Chem.* **1988**, *41*, 1963.

(38) Bard, A. J.; Faulkner, L. R. *Electrochemical Methods Fundamentals and Applications*, 2nd ed.; John Wiley and Sons: New York, 2001; p 36.

(39) We thank the reviewer who brought this to our attention.

(40) The 2nd reduction wave of **1**-NO_2 (corresponding to the reduction of the $-NO_2$ group) is also sensitive to C_{CH_3OH}. Analysis according to eqs 5 and 6 yields a slope of 116 mV (r^2 = 0.943), indicating that the $-NO_2^{\bullet-}$ group associates with ∼2 CH_3OH molecules. (The corresponding values for CD_3OD are slope = 105 mV and r^2 = 0.962.)

(41) (a) Whiddon, C.; Soderman, O. *Langmuir* **2001**, *17*, 1803. (b) Abildgaard, J.; Bolvig, S.; Hansen, P. E. *J. Am. Chem. Soc.* **1998**, *120*, 9063.

equilibrium constants for the [**1**-$NO_2^{\bullet-}$]$^-$···(m = 4)-(methanol) adducts are attributed to the high electrostatic charge density on the enolate oxygen (Scheme 3).

Conclusions

The facile synthesis of **1**-X's renders the 4-benzoylpyridinium system an attractive redox molecular building block. However, from a practical standpoint, chemical reversibility is of paramount importance for any redox system. In that regard, comparison of **1**-X's with viologens such as HV^{2+} has risen naturally (Figure 1A). In its most economically significant application (solution-phase electrochromic systems), HV^{2+} is cycled between the dicationic and the 1-e reduced form, $HV^{\bullet+}$.[19] But chemical stability of $HV^{\bullet+}$ or [**1**-X]$^\bullet$ is not sufficient, because disproportionation (eq 7) produces a very low concentra-

$$2[\mathbf{1}\text{-X}]^\bullet \rightleftarrows [\mathbf{1}\text{-X}]^- + [\mathbf{1}\text{-X}]^+ \qquad (7)$$

tion of HV° or of [**1**-X]$^-$. And, although [**1**-X]$^\bullet$ and $HV^{\bullet+}$ are stable species, it is also well-documented that in water both [**1**-X]$^-$ and the 2-e reduced form of viologen are not stable.[2,16] Since $\Delta E_{1/2}$ of **1**-X's is much wider than that of HV^{2+} (Figure 1A), the equilibrium concentration of HV° is calculated at about 10^4 times higher than that of [**1**-X]$^-$, under the same conditions. Therefore, based on thermodynamics alone, [**1**-X]$^\bullet$'s should be able to tolerate traces of water better than $HV^{\bullet+}$, and **1**-X's may be well-suited for applications analogous to those of HV^{2+}.

A second important ramification of this study stems from **1**-NO_2. Since $-NO_2^{\bullet-}$ is a strong electron donor, by reducing nitro−aromatic systems one may invert their reactivity. Currently, we are investigating Diels−Alder reactions of reduced nitrobenzene and 1-nitronaphthalene.

Experimental Section

Methods. All electrochemical experiments were carried out with an Au disk working electrode (1.6 mm in diameter, from Bioanalytical Systems, Inc., West Lafayette, IN), an aqueous Ag/AgCl reference electrode (also from BAS), and an Au foil (2.5 cm^2) as a counter electrode, in Ar-degassed anhydrous CH_3CN/0.1 M TBAP solutions at room temperature (23 ±1 °C). All voltammograms have been 80% compensated for solution resistance. For experiments involving addition of CD_3OD vs CH_3OH (Figures 3 and 4) we used a common stock solution of **1**-X, separated in two halves. All reactions were carried out under N_2 in flame-dried glassware. Melting points were uncorrected. Elemental analyses were performed by Oneida Research Services, Inc., Whiteboro, NY. Semiempirical calculations (PM3) were conducted with the Spartan Version 5.0.3 for SiliconGraphics software package (Wavefunction, Inc., Irvine, CA).

Materials. All starting materials, reagents, and solvents were commercially available and were used as received unless noted otherwise. Fc and BP-H were sublimed. TBAP was prepared as described before.[16] The synthesis of the free bases of **1**-Br, and **1**-C≡CH (i.e., BP-Br and BP-C≡CH) also has been described before.[16] The remaining free bases were synthesized as follows.

4-*(4*-Nitrobenzyl)pyridine.[23] 4-Benzylpyridine (8.0 mL, 0.05 mol) was added slowly to a cooled (∼10 °C) mixture of concentrated HNO_3 (17 mL) and concentrated H_2SO_4 (17 mL), so that the temperature of the reaction mixture does not rise above 20 °C. The reaction mixture was stirred at 10−20 °C for 1 h, subsequently was heated to ∼50 °C for 5 min, and then was poured into 100 g of ice. The resulting solution was pH adjusted to 8 with concentrated NH_4OH and extracted with diethyl ether. The combined organic layers were dried with anhydrous Na_2SO_4, the solvent was removed in vacuo, and the crude product was recrystallized from ethyl acetate to give 4-(4-nitrobenzyl)pyridine as off-white crystals. Yield 2.85 g (27%); mp 72−74 °C (lit.[23] mp 74 °C); ^{1}H NMR ($CDCl_3$, 400 MHz) δ 4.08 (2H, s, CH_2), 7.10 (2H, dd, $J_{2,6} = J_{3,5} = 1.6$ Hz, $J_{2,3} = J_{5,6} = 4.4$ Hz, H-2,6), 7.35 (2H, d, $J_{9,10} = J_{12,13} = 8.8$ Hz, H-9,13), 8.18 (2H, d, $J_{9,10} = J_{12,13} = 8.8$ Hz, H-10,12), 8.55 (2H, dd, $J_{2,6} = J_{3,5} = 1.6$ Hz, $J_{2,3} = J_{5,6} = 4.4$ Hz, H-3,5).

4-*(4*-Nitrobenzoyl)pyridine (BP-NO_2**)** was prepared via $KMnO_4$ oxidation of 4-(4-nitrobenzyl)pyridine according to the method by Muth et al.[24] Mp 123−124 °C (lit.[24] mp 118−121 °C); ^{1}H NMR ($CDCl_3$, 400 MHz) δ 7.57 (2H, dd, $J_{2,6} = J_{3,5} =$ 1.9 Hz, $J_{2,3} = J_{5,6} = 4.4$ Hz, H-2,6), 7.94−7.98 (2H, m, AA′XX′, H-9,13), 8.34−8.37 (2H, m, AA′XX′ H-10,12), 8.86 (2H, dd, $J_{2,6} = J_{3,5} = 1.9$ Hz, $J_{2,3} = J_{5,6} = 4.4$ Hz, H-3,5); ^{13}C NMR ($CDCl_3$, 100 MHz) δ 122.6, 123.8, 130.8, 140.7, 142.7, 150.3, 150.7, 193.4 (C═O).

4-(4-Methylbenzoyl)pyridine (BP-CH_3**)** was prepared from isonicotinic acid (15 g, 0.12 mol) and $SOCl_2$ (50 mL), followed by reaction of the isonicotinoyl chloride with toluene (80 mL) in the presence of $AlCl_3$ (30 g), according to the method used for BP-Br.[16] The crude product was recrystallized from hexane to yield BP-CH_3 as a white solid. Yield 9.8 g (42%); mp 94−95 °C (lit.[21b] mp 96−97 °C); ^{1}H NMR ($CDCl_3$, 400 MHz) δ 2.44 (3H, s, CH_3), 7.27−7.31 (2H, m, AA′XX′, H-10,12), 7.54 (2H, dd, $J_{2,3} = J_{5,6} = 4.3$ Hz, $J_{3,5} = J_{2,6} = 1.6$ Hz, H-2,6), 7.69−7.73 (2H, m, AA ′XX′, H-9,13), 8.78 (2H, dd, $J_{2,3} = J_{5,6} = 4.3$ Hz, $J_{3,5} = J_{2,6} = 1.6$ Hz, H-3,5); ^{13}C NMR ($CDCl_3$, 100 MHz) δ 21.7 (Me), 122.8, 129.3, 130.3, 133.2, 144.6, 144.7, 150.2, 194.7 (C═O).

4-(4-Formylbenzoyl)pyridine (BP-CHO**)** was prepared via a modification of the synthesis of *p*-nitrobenzaldehyde.[22] BP-CH_3 (2.0 g, 0.012 mol) was added to glacial acetic acid (15 mL) and acetic anhydride (15 mL). The solution was cooled in an ice bath and concentrated H_2SO_4 (4 mL) was added slowly. While the flask was still in the ice bath, CrO_3 (3 g, 0.03 mol) was added in portions to ensure that the temperature of the mixture never exceeded 10 °C. The cold mixture was stirred for another 30 min and was poured into ice (50 g). The pH of the resulting solution was raised to 8−9 with a 30% (w/v) K_2CO_3 solution, followed by extraction with CH_2Cl_2. The organic layers were collected, dried (Na_2SO_4), and evaporated to dryness. The residue was recrystallized from EtOH and dried under vacuum to give 4-[4-bis(acetyloxy)methylbenzoyl]pyridine as off-white crystals. Yield 1.18 g (37%); mp 120−122 °C; ^{1}H NMR ($CDCl_3$, 400 MHz) δ 2.14 (6H, s, CH_3), 7.56 (2H, dd, $J_{2,3} = J_{5,6} = 4.4$ Hz, $J_{3,5} = J_{2,6} = 1.6$ Hz, H-2,6), 7.64 (2H, br d, $J_{9,10} = J_{12,13} = 8.3$ Hz, H-10,12), 7.71 (1H, s, CH), 7.83 (2H, br d, $J_{9,10} = J_{12,13} = 8.3$ Hz, H-9,13), 8.80 (2H, dd, $J_{2,3} = J_{5,6} = 4.4$ Hz, $J_{3,5} = J_{2,6} = 1.6$ Hz, H-3,5); ^{13}C NMR ($CDCl_3$, 100 MHz) δ 20.7, 88.9, 122.7, 127.0, 130.3, 136.9, 140.4, 143.8, 150.4, 168.6 (C═O, acetyloxy), 194.4 (C═O, benzoyl). Anal. Calcd for $C_{17}H_{15}NO_5$: C, 65.17; H, 4.83; N, 4.47. Found: C, 64.88; H, 4.85; N, 4.34. Subsequently, 4-[4-bis(acetyloxy)-methylbenzoyl]pyridine (1 g, 3.19 mmol) was dissolved in EtOH/H_2O/concentrated H_2SO_4 (21 mL, 10:10:1, v/v/v) and was refluxed for 30 min. At the end of the period, the reaction mixture was allowed to cool to room temperature, the pH was adjusted to 8−9 with 30% (w/v) K_2CO_3, and the mixture was cooled in an ice bath. The precipitate was filtered, washed with water, and dried in vacuo to give BP-CHO as a white solid. Yield 0.51 g (76%); mp 122−123 °C; ^{1}H NMR ($CDCl_3$, 400 MHz) δ 7.58 (2H, dd, $J_{2,3} = J_{5,6} = 4.4$ Hz, $J_{3,5} = J_{2,6} = 1.6$ Hz, H-2,6), 7.92−7.96 (2H, m, AA ′XX′, H-10,12), 8.00−8.03 (2H, m, AA′XX′, H-9,13), 8.84 (2H, dd, $J_{2,3} = J_{5,6} = 4.4$ Hz, $J_{3,5} = J_{2,6} = 1.6$ Hz, H-3,5), 10.13 (1H, s, CHO); ^{13}C NMR ($CDCl_3$, 100 MHz) δ 122.7, 129.7, 130.5, 139.2, 140.5, 143.3, 150.6, 191.3 (CHO), 194.4 (C═O). Anal. Calcd for $C_{13}H_9NO_2$: C, 73.92; H, 4.29; N, 6.63. Found: C, 73.39; H, 3.74; N, 6.47.

4-(4-Methoxybenzoyl)pyridine (BP-OCH_3**)** was prepared from isonicotinic acid (5 g, 0.040 mol) and $SOCl_2$ (20 mL), followed by reaction of the isonicotinoyl chloride with anisole (30 mL) in the presence of $AlCl_3$ (10 g) according to the method used for BP-CH_3 above. Yield 3.2 g (38%); mp 119−121 °C (lit.[21b] mp 124 °C); ^{1}H NMR ($CDCl_3$, 400 MHz) δ 3.88 (3H, s, OCH_3), 6.95−6.98 (2H m, AA′XX′, H-10,12), 7.52 (2H, dd, $J_{2,3} = J_{5,6} = 6.0$ Hz, $J_{3,5} = J_{2,6} = 1.7$ Hz, H-2,6), 7.79−7.83 (2H, m, AA′XX′, H-9,13), 8.77 (2H, dd, $J_{2,3} = J_{5,6} = 6.0$ Hz, $J_{3,5} = J_{2,6} = 1.7$ Hz, H-3,5); ^{13}C NMR ($CDCl_3$, 100 MHz) δ 55.6 (OCH_3), 113.9, 122.7, 128.6, 132.7, 145.2, 150.2, 164.0, 193.7 (C═O).

4-(4-Methylthiobenzoyl)pyridine (BP-SCH_3**)** was prepared from isonicotinic acid (5 g, 0.040 mol) and $SOCl_2$ (20 mL), followed by reaction of the isonicotinoyl chloride with thioanisole (30 mL) in the presence of $AlCl_3$ (10 g) according to the method used for BP-CH_3 above. The crude product was recrystallized from CH_3OH to give off-white crystals. Yield 2.6 g (28%); mp 134−136 °C; ^{1}H NMR ($CDCl_3$, 400 MHz) δ 2.53 (3H, s, SCH_3), 7.27−7.31 (2H, m, AA′XX′, H-10,12), 7.53 (2H, br d, $J_{2,3} = J_{5,6} = 5.7$ Hz, H-2,6), 7.70−7.74 (2H, m, AA′XX′, H-9,13), 8.78 (2H, br d, $J_{2,3} = J_{5,6} = 5.7$ Hz, H-3,5); ^{13}C NMR ($CDCl_3$, 100 MHz) δ 14.7 (SCH_3), 122,7, 124.9, 130.6, 131.9, 144.7, 147.1, 150.3, 194.1 (C═O). Anal. Calcd for $C_{13}H_{11}NOS$: C, 68.09; H, 4.84; N, 6.11. Found: C, 68.19; H, 4.77; N, 5.98.

General Procedure for the Synthesis of 1-X Quaternary Salts. $(CH_3)_3OBF_4$ (1.0−1.8 equiv) dissolved in CH_3NO_2 (10 mL) was added dropwise to a solution of the corresponding free base (1 equiv) and the resulting solution was stirred at room temperature for 20 min. The crude product was precipitated by addition of diethyl ether, collected by vacuum filtration, and recrystallized from water to yield **1**-X as a white solid, unless indicated otherwise.

4-(4-Nitrobenzoyl)-*N*-methylpyridinium tetrafluoroborate (1-NO_2) was prepared from BP-NO_2 (0.90 g, 3.95 mmol). Yield 1.12 g (86%); mp 171−172 °C; ^{1}H NMR (CD_3CN, 400 MHz) δ 4.39 (3H, s, CH_3N^+), 7.97−8.01 (2H, m, AA′XX′, H-9,13), 8.20 (2H, br d, $J_{2,3} = J_{5,6} = 6.4$ Hz, H-2,6), 8.36−8.40 (2H, m, AA′XX′, H-10,12), 8.82 (2H, br d, $J_{2,3} = J_{5,6} = 6.4$ Hz, H-3,5); ^{13}C NMR (DMSO-d_6, 100 MHz) δ 48.2 (CH_3N^+), 123.9, 126.9, 131.5, 139.2, 146.6, 149.8, 150.5, 191.1 (C═O); UV−vis (CH_3CN) λ_{max}, nm (ϵ, M^{-1} cm^{-1}) 227 (11 000), 271 (18 600). Anal. Calcd for $C_{13}H_{11}N_2O_3BF_4$: C, 47.31; H, 3.36; N, 8.49. Found: C, 47.30; H, 3.00; N, 8.61.

4-(4-Methylbenzoyl)-*N*-methylpyridinium tetrafluoroborate (1-CH_3) was prepared from BP-CH_3 (1.00 g, 5.08 mmol). Yield 1.28 g (84%); mp 162−164 °C; ^{1}H NMR (DMSO-d_6, 400 MHz) δ 2.43 (3H, s, CH_3), 4.42 (3H, s, CH_3N^+), 7.42−7.46 (2H, m, AA′XX′, H-10,12), 7.70−7.74 (2H, m, AA′XX′, H-9,13), 8.31 (2H, d, $J_{2,3} = J_{5,6} = 6.6$ Hz, H-2,6), 9.16 (2H, d, $J_{2,3} = J_{5,6} = 6.6$ Hz, H-3,5); ^{13}C NMR (DMSO-d_6, 100 MHz) δ 21.3 (Me), 48.1 (CH_3N^+), 126.4, 129.7, 130.4, 131.7, 145.8, 146.4, 151.7, 191.7 (C═O); UV−vis (CH_3CN) λ_{max}, nm (ϵ, M^{-1} cm^{-1}) 232 (10 100), 227 (9 300). Anal. Calcd for $C_{14}H_{14}NOBF_4$: C, 56.22; H, 4.68; N, 4.68. Found: C, 56.11; H, 4.71; N, 4.60.

4-Benzoyl-*N*-methylpyridinium tetrafluoroborate (1-H) was prepared from BP-H (Aldrich, 1.00 g, 5.46 mmol). Yield 0.91 g (58%); mp 170−171 °C (lit.[42] mp 168 °C); ^{1}H NMR (DMSO-d_6, 400 MHz) δ 4.43 (3H, s, CH_3N^+), 7.61−7.66 (2H, m, H-10,12), 7.77−7.84 (3H, m, H-9,11,13), 8.33 (2H, d, $J_{2,3} = J_{5,6} = 6.6$ Hz, H-2,6), 9.17 (2H, d, $J_{2,3} = J_{5,6} = 6.6$ Hz, H-3,5); ^{13}C NMR (DMSO-d_6, 100 MHz) δ 48.1 (CH_3N^+), 126.5, 129.1, 130.2, 134.2, 134.8, 146.5, 151.3, 192.2 (C═O); UV−vis (CH_3CN) λ_{max}, nm (ϵ, M^{-1} cm^{-1}) 225 (13 500), 270 (11 300).

4-(4-Formylbenzoyl)-*N*-methylpyridinium tetrafluoroborate (1-CHO) was prepared from BP-CHO (0.48 g, 2.27 mmol). Yield 0.61 g (86%); mp 181−182 °C; ^{1}H NMR (DMSO-d_6, 400 MHz) δ 4.44 (3H, s, CH_3N^+), 8.00 (2H, br d, $J_{9,10} = J_{12,13} = 8.2$ Hz, H-10,12), 8.13 (2H, br d, $J_{9,10} = J_{12,13} = 8.2$ Hz, H-9,13), 8.36 (2H, d, $J_{2,3} = J_{5,6} = 6.6$ Hz, H-2,6), 9.19 (2H, d, $J_{2,3} = J_{5,6} = 6.6$ Hz, H-3,5), 10.17 (1H, s, CHO); ^{13}C NMR (DMSO-d_6, 100 MHz) δ 48.2 (CH_3N^+), 126.7, 129.7, 130.8, 138.4, 139.5, 146.6, 150.4, 191.8 (C═O), 193.0 (CHO); UV−vis (CH_3CN) λ_{max}, nm (ϵ, M^{-1} cm^{-1}) 233 (11 200), 273 (18 300). Anal. Calcd for $C_{14}H_{12}NO_2BF_4$: C, 53.71; H, 3.86; N, 4.47. Found: C, 53.46; H, 3.39; N, 4.42.

4-(4-Methoxylbenzoyl)-*N*-methylpyridinium tetrafluoroborate (1-OCH_3) was prepared from BP-OCH_3 (0.80 g, 3.76 mmol). Yield 0.70 g (59%); mp 142−143 °C;^{1}H NMR (DMSO-d_6, 400 MHz) δ 3.89 (3H, s, OCH_3), 4.41 (3H, s, CH_3N^+), 7.13−7.17 (2H, m, AA′XX′, H-10,12), 7.78−7.82 (2H, m, AA′XX′, H-9,13), 8.30 (2H, d, $J_{2,3} = J_{5,6} = 6.6$ Hz, H-2,6), 9.15 (2H, d, $J_{2,3} = J_{5,6} = 6.6$ Hz, H-3,5); ^{13}C NMR (DMSO-d_6, 100 MHz) δ 48.1 (CH_3N^+), 55.9 (OCH_3), 114.5, 126.2, 127.0, 132.8, 146.4, 152.1, 164.6, 190.5 (C═O); UV−vis (CH_3CN) λ_{max}, nm (ϵ, M^{-1} cm^{-1}) 208 (18 300), 258 (10 500), 304 (7 ,900). Anal. Calcd for $C_{14}H_{14}NO_2BF_4$: C, 53.37; H, 4.48; N, 4.45. Found: C, 53.20; H, 4.04; N, 4.40.

4-(4-Methylthiobenzoyl)-*N*-methylpyridinium tetrafluoroborate (1-SCH_3) was prepared as a yellow solid from BP-SCH_3 (0.51 g, 0.22 mol) and exactly 1 equiv of $(CH_3)_3OBF_4$. Yield 0.61 g (85%); mp 168−169 °C;^{1}H NMR (DMSO-d_6, 400 MHz) δ 2.57 (3H, s, SCH_3), 4.41 (3H, s, CH_3N^+), 7.42−7.48 (2H, m, AA′XX′, H10,12), 7.70−7.75 (2H, m, AA′XX′, H9,13), 8.31 (2H, d, $J_{2,3} = J_{5,6} = 6.6$ Hz, H2,6), 9.17 (2H, d, $J_{2,3} = J_{5,6} = 6.6$ Hz, H3,5); ^{13}C NMR (CD_3CN, 100 MHz) δ 14.7 (SCH_3), 49.5 (CH_3N^+), 118.3, 126.0, 128.0, 131.3, 131.6, 147.2, 150.1, 153.5, 191.6 (C═O); UV−vis (CH_3CN) λ_{max}, nm (ϵ, M^{-1} cm^{-1}) 219 (13 500), 275 (10 700), 341 (10 400). Anal. Calcd for $C_{14}H_{14}NOSBF_4$: C, 50.78; H, 4.26; N, 4.23. Found: C, 50.54; H, 4.20; N, 4.17.

4-(4-Dimethylsulfoniumbenzoyl)-*N*-methylpyridinium bis(tetrafluoroborate) (1-$^+S(CH_3)_2$) was prepared from **1**-SCH_3 (0.27 g, 0.81 mmol) and 1.5 equiv of $(CH_3)_3OBF_4$. At the end of the reaction period, CH_3OH (1 mL) was added to quench the excess of $(CH_3)_3OBF_4$ and the solution was evaporated to dryness to give a pale yellow gum-like solid. Yield 0.31 g (88%); ^{1}H NMR (DMSO-d_6, 400 MHz) δ 3.32 (6H, s, $S(CH_3)_2$), 4.44 (3H, s, CH_3N^+), 8.05−8.08 (2H, m, AA′XX′, H-10,12), 8.25−8.28 (2H, m, AA′XX′, H-9,13), 8.33 (2H, d, $J_{2,3} = J_{5,6} = 6.7$ Hz, H-2,6), 9.19 (2H, d, $J_{2,3} = J_{5,6} = 6.7$ Hz, H-3,5); ^{13}C NMR (CD_3CN, 100 MHz) δ 28.9 (CH_3S^+), 49.7 (CH_3N^+), 118.9, 128.3, 131.4, 132.8, 139.7, 147.7, 151.0, 192.1 (C═O); UV−vis (CH_3CN) λ_{max}, nm (ϵ, M^{-1} cm^{-1}) 228 (13 000), 260 (11 600). Anal. Calcd for $C_{15}H_{17}NOSB_2F_8$: C, 41.61; H, 3.96; N, 3.23. Found: C, 41.11; H, 3.84; N, 3.24.

4-(4-Bromobenzoyl)-*N*-methylpyridinium tetrafluoroborate (1-Br) was prepared from BP-Br (2.35 g, 8.97 mmol).[16] Recrystallized from ethanol to white needles. Yield 2.52 g (77%); mp 147−148 °C; ^{1}H NMR (CD_3CN, 400 MHz) δ 4.40 (3H, s, CH_3N^+), 7.69−7.73 (2H, m, AA′XX′, H-10,12), 7.79 (2H, m, AA′XX′, H-9,13), 8.16 (2H, d, $J_{2,3} = J_{5,6} = 6.4$ Hz, H-2,6), 8.82 (2H, d, $J_{2,3} = J_{5,6} = 6.4$ Hz, H-3,5); ^{13}C NMR (CD_3CN, 100 MHz) δ 49.6, 128.2, 130.6, 132.9, 133.4, 134.4, 147.5, 152.5, 192.0 (C═O); UV−vis (CH_3CN) λ_{max}, nm (ϵ, M^{-1} cm^{-1}) 228 (13 500), 278 (12 300).

4-(4-Ethynylbenzoyl)-*N*-methylpyridinium tetrafluoroborate (1-C≡CH) was prepared from BP-C≡CH (1.00 g, 4.83 mmol).[16] Yield 1.25 g (84%); mp 229−231 °C dec; ^{1}H NMR (CD_3CN, 400 MHz) δ 3.73 (1H, s, acetylenic), 4.40 (3H, s, CH_3N^+), 7.68−7.72 (2H, m, AA′XX′, H-10,12), 7.78−7.82 (2H, m, AA′XX′, H-9,13), 8.17 (2H, d, $J_{2,3} = J_{5,6} = 6.4$, H-2,6), 8.81 (2H, d, $J_{2,3} = J_{5,6} = 6.4$, H-3,5); ^{13}C NMR (CD_3CN, 100 MHz) δ 49.7, 83.0, 83.5, 128.3, 129.3, 131.4, 133.6, 135.3, 147.4, 152.6, 192.1 (C═O); UV−vis (CH_3CN) λ_{max}, nm (ϵ, M^{-1} cm^{-1}) 249 (10 900), 288 (12 300).

4-Acetyl-*N*-methylpyridium tetrafluoroborate (*N*-MeAP$^+$) was prepared from 4-acetylpyridine (AP, 1.03 g, 0.84 mol). Yield 1.70 g (90%); mp 107−109 °C (lit.[42] mp 105−107 °C); ^{1}H NMR (DMSO-d_6, 400 MHz) δ 2.73 (3H, s, $COCH_3$), 4.40 (3H, s, CH_3N^+), 8.45 (2H, d, $J_{2,3} = J_{5,6} = 6.6$, H-2,6), 9.16 (2H, d, $J_{2,3} = J_{5,6} = 6.6$, H-3,5); ^{13}C NMR (DMSO-d_6, 100 MHz) δ

(42) Burke, M. R.; Brown, T. L. *J. Am. Chem. Soc.* **1989**, *111*, 5185.

27.3, 48.2, 125.5, 147.0, 148.1, 195.7 (C═O); UV−vis (CH_3CN) λ_{max}, nm (ϵ, M^{-1} cm^{-1}) 224 (9 350), 275 (3 900), 336 (sh); IR (KBr) (ν, cm^{-1}) 1698 (C═O), 1640 (CH_3-N^+).

Acknowledgment. We gratefully acknowledge support from the Petroleum Research Fund, administered by the ACS (Grant No. 35154-AC5), and from the National Cancer Institute (Grant No.1 R15 CA82141-01A2 to C.S.-L.).

Supporting Information Available: Scheme S.1, Synthesis of the 4-(*p*-substituted benzoyl)-*N*-methylpyridinium tetrafluoroborate salts (**1**-X); Figure S.1, HLFE plot for the 4-benzoylpyridine free bases; Table S.1, IR stretching frequencies of C═O and N^+-CH_3 as a function of substitution; Figure S.2, correlation of the IR stretching frequencies of **1**-X's with the σ_{p-X} values. This material is available free of charge via the Internet at http://pubs.acs.org.

JO020489+